Mon. Not. R. Astron. Soc. **275**, L47–L51 (1995)

HST observations of three radio galaxies at redshift $z \approx 1$

M. S. Longair,[1] P. N. Best[1] and H. J. A. Röttgering[1,2]
[1] *Cavendish Laboratory, Madingley Road, Cambridge CB3 0HE*
[2] *Institute of Astronomy, Madingley Road, Cambridge CB3 0HA*

Accepted 1995 June 6. Received 1995 February 27; in original form 1995 January 11

ABSTRACT

The first results of a programme to image a sample of radio galaxies at redshift $z \approx 1$ with the *Hubble Space Telescope* are reported in this Letter. The images of the three galaxies presented here (3C 368, 3C 324 and 3C 265) show a wealth of fine structure down to the resolution limit of the *HST*. All three systems show a clear alignment of the optical emission with the axis of the double radio source, a phenomenon first noted by Chambers et al. and McCarthy et al. The appearance of the alignment is, however, quite different in each case. It is argued that the remarkable structures seen in the *HST* images are different manifestations of activity associated with the radio source phenomenon, with the alignment effects being a result of at least two different mechanisms.

Key words: galaxies: active – galaxies: individual: 3C 368 – galaxies: individual: 3C 324 – galaxies: individual: 3C 265 – infrared: galaxies – radio continuum: galaxies.

1 INTRODUCTION

Radio galaxies are the most extensively studied stellar systems that can be observed at large redshifts. The best-studied sample of radio galaxies is that belonging to the 3CR catalogue (Laing, Riley & Longair 1983). The radio, optical and infrared properties of these radio galaxies exhibit strong evolutionary changes with cosmic epoch (Lilly & Longair 1984). These objects are therefore of special importance for understanding the evolution, with cosmic epoch, of active galaxies in general.

To understand the nature of these active systems, a complete sample of 28 3CR radio galaxies has been selected, which lie in the region of sky $|b| \geq 10°$, $10° \leq |\delta| \leq 60°$, and which have redshifts in the range $0.6 \leq z \leq 1.8$. In this Letter, we report the first results of a programme to image this sample of radio galaxies using the *Hubble Space Telescope* (*HST*), in conjunction with new high-resolution radio observations made with the Very Large Array (VLA). Images of 3C 368 ($z = 1.13$), 3C 324 ($z = 1.21$) and 3C 265 ($z = 0.81$) taken with the Wide Field and Planetary Camera 2 (WFPC2) are presented. These images are amongst the most spectacular of the sample to date, although the majority of the galaxies in the sample do exhibit intriguing structures.

2 OBSERVATIONS

HST images of each object were taken in two different filters for about half an hour each; details of the observations are given in Table 1. The data were reduced using the standard STScI reduction pipeline (Lauer 1989). The sources have also been observed at 8 GHz with the VLA radio synthesis telescope in A-array configuration, giving a spatial resolution of 0.15 arcsec, comparable to the 0.1-arcsec resolution of the *HST* images. The VLA observations consisted of 22-min exposures giving an rms noise level of about 50 μJy. The radio data were reduced using the standard AIPS software provided by NRAO (Perley 1989).

HST images of the three radio galaxies, with the high-resolution radio maps superimposed, are shown in Figs 1, 3 and 5 (see Sections 2.1–2.3). The absolute positioning of the optical frames was found using one or more unsaturated stars which were present on each frame and which were also present in the APM data base (Maddox et al. 1990). The astrometric error is typically 0.5 to 1.0 arcsec. Thus, in the present analysis, the positional accuracy in aligning the images is significantly poorer than the resolution of the VLA and *HST* observations.

2.1 3C 368

3C 368 is one of the best-studied radio galaxies at a redshift $z \sim 1$ (e.g. Djorgovski et al. 1987; Chambers, Miley & Joyce 1988; Scarrott, Rolph & Tadhunter 1990; Hammer, Le Fèvre & Proust 1991). The *HST* image (Fig. 1) shows a remarkable 'cigar-shaped' emission region, oriented along the main radio axis. The bright unresolved knot close to the centre of this emission region is a foreground M-dwarf star, identified by Hammer et al. (1991). Our 8-GHz radio image shows no evidence for a radio core to a flux density limit of

Table 1. The parameters of the *HST* observations. The source name is given in column (1), and its redshift in column (2). Column (3) gives the WFPC2 filter used for the observation, with the central wavelength and width of the filter in ångstroms being given in columns (4) and (5). Column (6) is the exposure time in seconds. Column (7) details contaminating lines in the filter, and column (8) gives an estimate of their average contamination based upon the line luminosities from references in column (9). References: A – Djorgovski et al. (1987); B – Scarrott et al. (1990); C – Hammer et al. (1991); D – Spinrad & Djorgovski (1984); E – Smith et al. (1979).

Source	z	Filter	Centre Å	Width Å	Exp. Time sec.	Contaminating Lines	% contam.	Refs
(1)	(2)	(3)	(4)	(5)	(6)	(7)	(8)	(9)
3C368	1.13	f702W	6900	1360	1700	[OII] 3727, [NeIII] 3869	~ 25%	A,B,C
		f791W	7830	1200	1800	[OII] 3727, [NeIII] 3869	~ 40%	A,B,C
3C324	1.21	f702W	6900	1360	1700	[OII] 3727, MgII 2799	~ 9%	D
		f791W	7830	1200	1800	[OII] 3727, [NeIII] 3869	~ 26%	D
3C265	0.81	f555W	5450	1230	1700	[NeV] 3346,3426	~ 2%	E
		f785LP	8650	1360	1700	[OIII] 5007	< 10%	E

50 μJy. This observation is in contrast to the 5-GHz observation of Chambers et al. (1988), who found a weak central radio component. If the latter observation is indeed a detection of the central radio core, the core must be highly variable.

Fig. 1 bears little resemblance to a giant elliptical galaxy, and so observations in the infrared K band at 2.2 μm were made to study the relatively old population of stars which could be associated with the elliptical galaxy hosting the active galactic nucleus (AGN). A 54-min exposure of 3C 368 in the K band was obtained with the infrared camera IRCAM3 on the United Kingdom Infrared Telescope (UKIRT) in 1994 August, in 1.0-arcsec seeing. Further analysis of this image will follow elsewhere, but for the moment we merely use it to pinpoint the centre of the galaxy. A cut made along the axis of the infrared image is shown in Fig. 2. Subtracting the unresolved M star, we identify the residual object with the extended continuum emission of the parent radio galaxy. It is centred 1 arcsec to the north of the M star, close to the bright emission region in Fig. 1, and we therefore propose that this is the centre of the galaxy.

An optical jet-like feature links this proposed centre with the emission regions in the northern part of the image. The northern radio component lies beyond these emission regions, suggesting that the optical jet and the other complex structures have been caused by the passage of the jet responsible for the intense radio emission. To the south of the M star, the radio component lies towards the leading edge of a roughly elliptical optical emission region. The clear intensity minimum in the centre of this part of the image indicates that the optical emission originates from an ellipsoidal shell resembling that found in bow-shocks (Meisenheimer & Hippelein 1992). An arc-shaped structure in PKS 2250−41, at a redshift $z = 0.3$, has recently been similarly associated with a bow-shock by Tadhunter et al. (1994).

No current theory of the alignment effect can solely account for all of the properties of the optical emission from 3C 368. The source is highly polarized optically (Scarrott et al. 1990; Cimatti et al. 1993), and the polarization properties indicate that at least a proportion of the extended aligned emission is scattered light from an obscured active galactic nucleus (Fabian 1989; Scarrott et al. 1990). For the case of uniformly distributed scatterers, the emission region would be expected to have a cone-like structure. The fact that

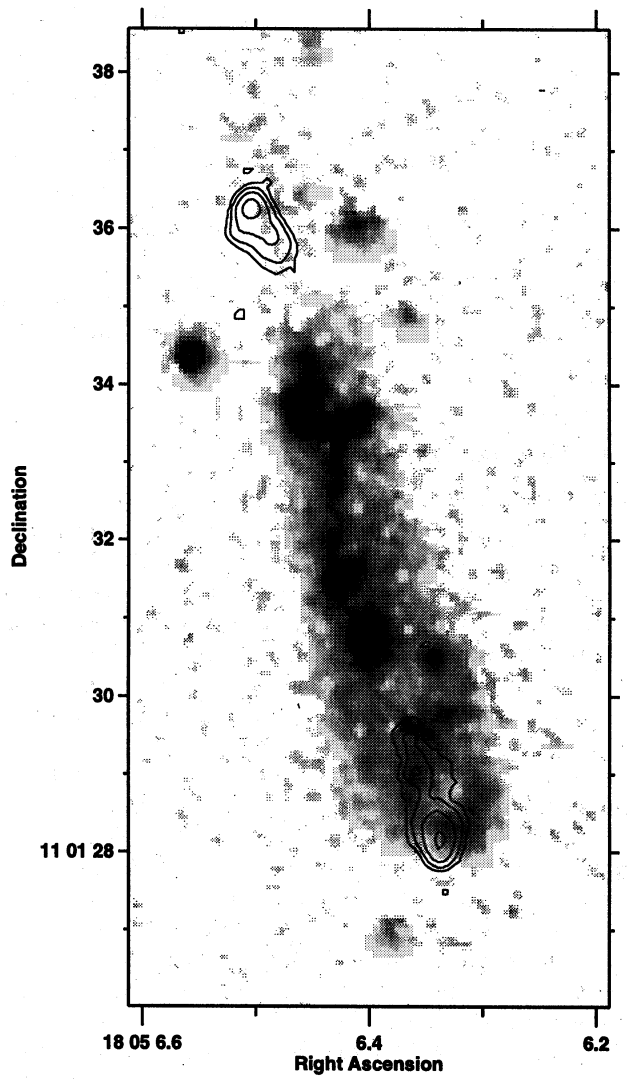

Figure 1. 3C 368: the image is the sum of both filters of the WFPC2 observations. The VLA data are superimposed, the contour levels being at $(1, 4, 16, 64) \times 1.18 \times 10^{-4}$ Jy beam^{-1}.

3C 368, and the other images presented here, does not have this simple structure indicates that one or more additional processes have to be invoked to explain the structure of the extended emission.

There is clearly a concentration of scattering material along the radio axis. This may be due to a pre-existing elongation of material around the radio galaxy (Eales 1992; West 1994; Röttgering et al. 1995), or may alternatively be a direct result of the radio source phenomenon. It has been argued that the passage of powerful radio jets induces massive star formation (McCarthy et al. 1987; Chambers et al. 1988; Begelman & Cioffi 1989; Rees 1989). In addition to the contribution of young stars to the alignment effect, dust associated with this star formation will result in an excess of scattering material along the radio axis. Given that the scalesize of the optical emission is similar to that of the radio structure, we favour this model; the knotty structures in the north of the galaxy would represent massive star-forming regions. In addition, we suggest that part of the southern structure of 3C 368 may be identified with a 'bow-shock' associated with the passage of the beam powering the radio source component.

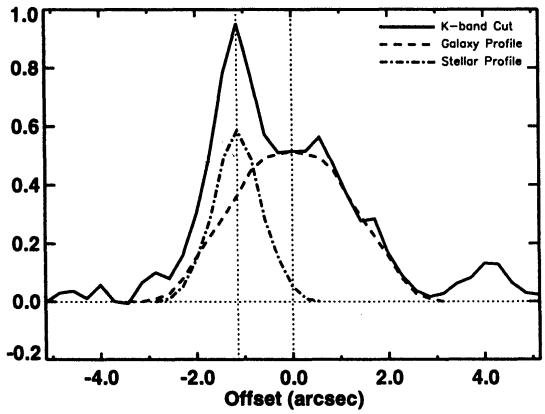

Figure 2. A cut along the axis of 3C 368 in the 2.2-μm *K* waveband. The *y*-axis shows intensity relative to the peak intensity, and error bars are ±0.003. The intensity distribution has been decomposed into the M star (dot–dash line) and the residual parent galaxy (dashed line). The centre of the galaxy lies just over 1 arcsec north of the M star.

2.2 3C 324

The image of 3C 324 (Fig. 3) is much clumpier than that of 3C 368 and appears to consist of a number of 'interacting' components. In contrast, a 54-min infrared *K*-band image obtained with IRCAM3 on UKIRT in 1-arcsec seeing has the appearance of a giant elliptical galaxy. This was registered with the *HST* image using unresolved stars that were present in both frames. It will be discussed in more detail elsewhere; here we compare only the distributions of emission along the radio axis in the two images. The *HST* image was convolved to 1-arcsec resolution and a cut made along the axis. The optical emission is 'flat-topped' (see Fig. 4), whilst a cut along the infrared image shows a central maximum, situated between the eastern and western components of the *HST* image (labelled 'A' and 'B' respectively in Fig. 3). This suggests that the optical image is strongly influenced by dust extinction.

The axis of the optical structures is misaligned by 30° with respect to the radio axis as defined by the outer radio hotspots, but it is aligned with an axis connecting the southern emission of the western lobe and the northern emission of the eastern lobe. This is the axis along which the transport of relativistic material is supposed to take place; radio structures associated with this axis are clearly present in the lower resolution VLA images at 5 GHz (Fernini et al. 1993).

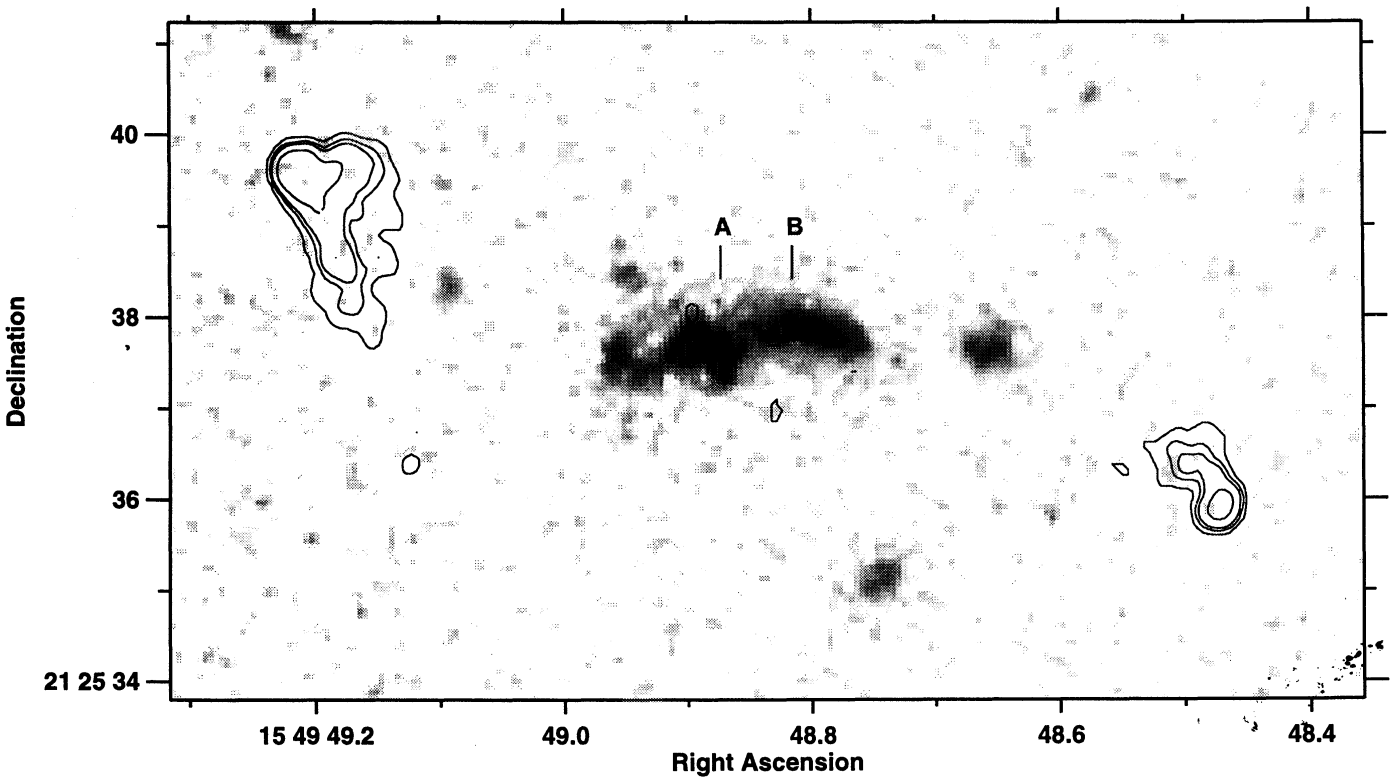

Figure 3. 3C 324: the image is the sum of both filters of the WFPC2 observations. The VLA data are superimposed, the contour levels being at $(2, 8, 16, 64) \times 1.18 \times 10^{-4}$ Jy beam^{-1}.

Unlike 3C 368, there is no clear association between the radio hotspots and the optical structures. If the optical emission regions are associated with companion galaxies, the alignment of these with the radio jet direction is striking and may be consistent with the model proposed by West (1994). In this model, the alignment is associated with anisotropic mergers during the formation of massive galaxies. A prolate galaxy is formed with its major axis pointing along the large-scale matter distribution. According to the model, the spin axis of a central black hole and hence the radio axis should also have the same orientation. The alignment effect is expected to be present on scales from tens of parsecs up to megaparsecs. It is of note, therefore, that the *HST* images fail to show a significant excess of galaxies along the radio axis further than 100 kpc from the centre.

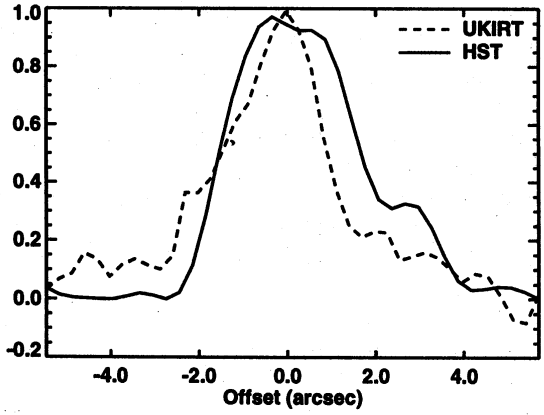

Figure 4. Cuts made along the axis of 3C 324. The solid line represents the sum of both filters of the WFPC2 observations. The dashed line is the UKIRT *K*-waveband image. The *y*-axis is intensity relative to the peak intensity. Error bars on the above diagram are ±0.002 for the *HST* cut, and ±0.003 for UKIRT.

In 3C 324, as in 3C 368, the contribution of line emission to the optical image is large (see Table 1), and could affect the overall structure. For both galaxies, however, the width-to-length ratio of the optical image is approximately 1:5 and the flux density is fairly uniformly distributed. For an upper limit to the line emission of 40 per cent (see Table 1), even in the unlikely case that all the line emission originates from the outer edges of the source, the continuum would still be aligned with a width-to-length ratio of 1:3. Thus the optical alignment of the galaxy cannot be wholly attributed to aligned line emission (cf. Meisenheimer & Hippelein 1992).

Le Fèvre et al. (1987) suggested that the alignment of 3C 324, and possibly of other sources, is due to gravitational lensing by a foreground object. None of the structures seen in the *HST* images suggests that this is the case.

2.3 3C 265

The radio galaxy associated with 3C 265 is surrounded by numerous emission regions or companion dwarf galaxies (Fig. 5). The radio structure is a factor of 10 more extended than the optical emission, and its direction is indicated by the lines in Fig. 5. At first glance, the optical structures have little

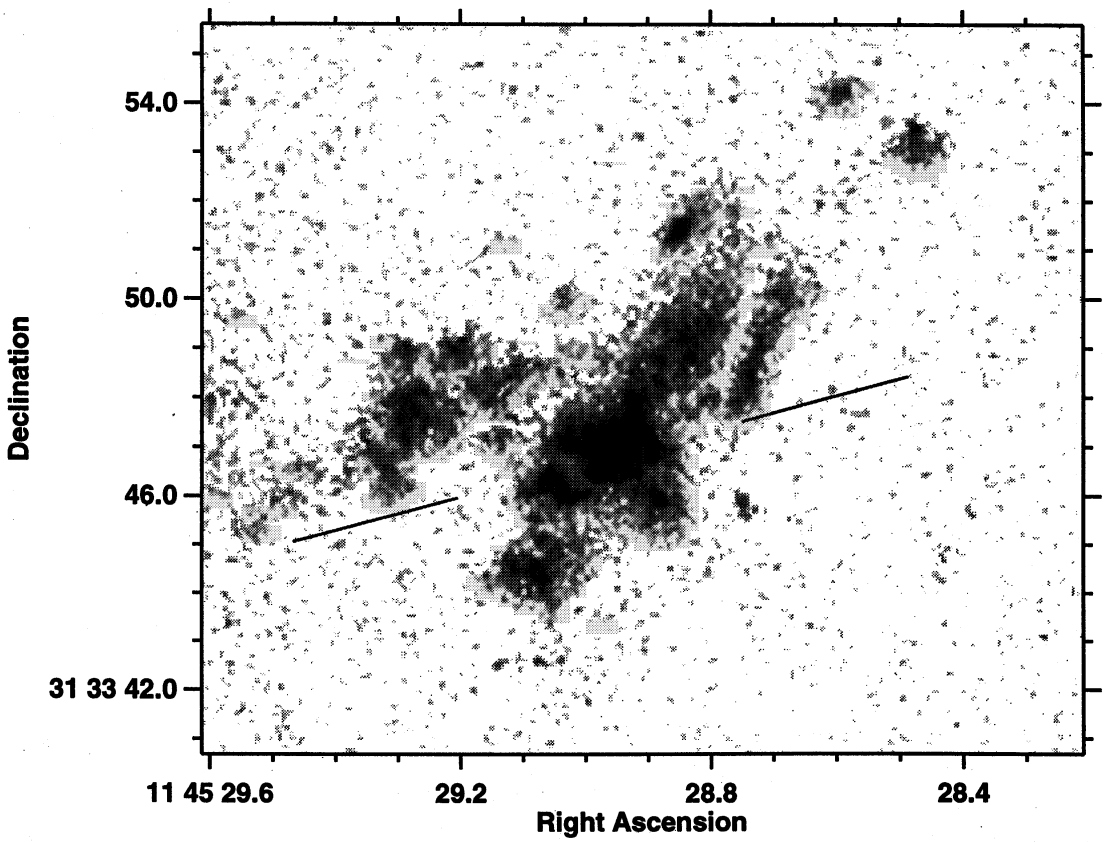

Figure 5. 3C 265: the image is the sum of the two filters of the WFPC2 observations. The radio axis is marked by lines.

apparent association with the double radio source. If, however, the *HST* image is convolved to a resolution of 3 arcsec, the optical axis, as determined from a Gaussian fit to the convolved *HST* image, is aligned within 25° of the radio axis.

These diffuse optical structures may be the result of a dynamical interaction between merging galaxies, producing regions of massive star formation. The luminosity of such regions might be enhanced by jet-induced star formation or by scattering, giving rise to a rough alignment of the optical and radio axes. Alternatively, the diffuse emission may be associated with large-scale gas clouds, possibly forming from massive cooling flows ($\sim 1000\ M_\odot\ yr^{-1}$) associated with the X-ray gas of a cluster around the giant elliptical galaxy (cf. 3C 356: Crawford & Fabian 1993). 3C 265 is among the most luminous radio galaxies known (Laing et al. 1983), and the fact that the radio structure extends to such large distances beyond the galaxy suggests that there must be confining gas which extends to a large radius about the radio galaxy. The emission regions may be associated with gas that has been compressed by the passage of the radio beam, and is cooling out of the X-ray halo. Such a picture would have important consequences for the evolution of giant elliptical galaxies because the cooling gas eventually falls on to the central galaxy, a process which may be important in the formation of giant cD galaxies. Given that the diffuse extended emission is strongly present in the WFPC2 f555W filter which contains no major emission lines, it must be predominantly continuum emission.

3 DISCUSSION

All three radio galaxy images presented here are aligned with the radio structure, but the sizes of the radio structures relative to the optical images are quite different. The galaxies have been discussed in order of increasing radio linear size. In the case of 3C 368 there is direct evidence for interaction between the radio jets and the ambient medium in the immediate vicinity of the galaxy, whereas in the case of 3C 265 the image indicates the aftermath of the passage of the radio beam. It seems likely that the alignments found in the three sources represent effects occurring at different phases in the evolution of the radio sources. We infer that there is no simple origin of the alignment effect, but rather that it is the result of different manifestations of the interaction of intense radio jets from an active galactic nucleus with its immediate environment. To understand fully the relative importance of these effects at different stages in the evolution of the radio galaxies, the sources need to be studied at *HST* resolution, not only in widely different colours, but also by polarimetry.

ACKNOWLEDGMENTS

This work is based on observations with the NASA/ESA *Hubble Space Telescope*, obtained at the Space Telescope Science Institute, which is operated by AURA, Inc., under contract with NASA. The National Radio Astronomy Observatory is operated by AURA, Inc., under co-operative agreement with the National Science Foundation. The United Kingdom Infrared Telescope is operated by the Royal Observatory Edinburgh. PNB acknowledges support from PPARC. HJAR acknowledges support from an EEC twinning project. We thank the referee for very helpful comments.

REFERENCES

Begelman M. C., Cioffi D. F., 1989, ApJ, 345, L21
Chambers K. C., Miley G. K., van Breugel W. J. M., 1987, Nat, 329, 604
Chambers K. C., Miley G. K., Joyce R. R., 1988, ApJ, 329, L75
Cimatti A., di Serego Alighieri S., Fosbury R. A. E., Salvati M., Taylor D., 1993, MNRAS, 264, 421
Crawford C. S., Fabian A. C., 1993, MNRAS, 260, L15
Djorgovski S., Spinrad H., Pedelty J., Rudnick L., Stockton A., 1987, AJ, 93, 1307
Eales S. A., 1992, ApJ, 397, 49
Fabian A. C., 1989, MNRAS, 238, 41P
Fernini I., Burns J. O., Bridle A. H., Perley R. A., 1993, AJ, 105, 1690
Hammer F., Le Fèvre O., Proust D., 1991, ApJ, 374, 91
Laing R. A., Riley J. M., Longair M. S., 1983, MNRAS, 204, 151
Lauer T. R., 1989, PASP, 101, 445
Le Fèvre O., Hammer F., Nottale L., Mathez G., 1987, Nat, 326, 268
Lilly S. J., Longair M. S., 1984, MNRAS, 211, 833
McCarthy P. J., van Breugel W. J. M., Spinrad H., Djorgovski S., 1987, ApJ, 321, L29
Maddox S. J., Sutherland W. J., Efstathiou G., Loveday J., 1990, MNRAS, 243, 692
Meisenheimer K., Hippelein H., 1992, A&A, 264, 455
Perley R. A., 1989, in Perley R. A., Schwab F. R., Bridle A. H., eds, ASP Conf. Ser. Vol. 6, Synthesis Imaging in Radio Astronomy. Astron. Soc. Pac., p. 287
Rees M. J., 1989, MNRAS, 239, 1P
Röttgering H. J. A., West M. J., Miley G. K., Chambers K. C., 1995, A&A, in press
Scarrott S. M., Rolph C. D., Tadhunter C. N., 1990, MNRAS, 243, 5P
Smith H. E., Junkkarinen V. T., Spinrad H., Grueff G., Vigotti M., 1979, ApJ, 231, 307
Spinrad H., Djorgovski S., 1984, ApJ, 280, L9
Tadhunter C., Shaw M., Clark N., Morganti R., 1994, A&A, 288, L21
West M. J., 1994, MNRAS, 268, 79